

ELECTRON-IMPACT DISSOCIATION AND IONIZATION CHANNELS IN H_2

O. J. Orient and A. Chutjian

Jet Propulsion Laboratory, California Institute of Technology

Pasadena, CA 91109 USA

ABSTRACT

Dissociative electron attachment (DA) to H_2 has been studied by measuring the outgoing kinetic energies of the H^- with H in the various final channels. The electron energies E_e studied are 3-30 eV. Effects of vibration-rotation population in H_2 are seen, and the DA results herein are modeled in terms of known cross sections for attachment from $H_2(v'',J'')$. In addition to the DA channels, characteristic ion energies corresponding to three other channels have been measured: direct ionization to H_2^+ has been detected at energies above that threshold (15.426 eV above the $H_2 v'' = J'' = 0$ ground state); ion-pair production has been measured by detecting the H^+ and H at energies E_e greater than that threshold of 17.322 eV; and dissociative ionization has been measured corresponding to E_e greater than 18,076 eV. Use is made of magnetically-confined electron and ion beams with trochoidal deflection to measure outgoing ion energies. Detection of positive- and negative-ion currents is through analog detection (Faraday cup) and charge digitization,

PACS Numbers: 34.80 Gs, 82.80, Fk

1. INTRODUCTION

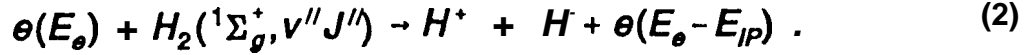
The study of low-energy electron scattering from molecular H_2 is critical to the understanding of the basic properties of this system, such as resonance phenomena and cross sections [1-7], and potential-energy curves and their asymptotic limits [8-14]. These data are also required to accounting correctly for the processes active in hydrogen negative-ion discharges [15-17]. For example, the observation of hydrogen-atom wall recombination to produce vibrationally-excited H_2 molecules within a hydrogen plasma is relevant to the modeling of these high-brightness ion sources, and was also quite unexpected [19-22].

The present work deals with measurements in four significant dissociation channels in H_2 : dissociative attachment (DA), ion-pair (IP) formation, dissociative ionization (DI), and direct ionization. By analysis of the kinetic energy of the ionic fragments, one is also able to identify the electronic state of the neutral (undetected) fragment [23]. Because of the very large variation of DA cross section with the H_2 ground vibrational state [3,9-11], one is also able to see clear effects of attachment to molecules which are in excited vibration-rotation levels of the $X^1\Sigma_g^+$ ground electronic state. These levels appear to be populated by the same mechanism as observed earlier, namely dissociation of the H_2 to H atoms by a hot electron-gun filament, followed by wall adsorption, recombination, and release of $H_2(v'', J'')$ into the collision region.

The negative-ion reaction channels studied are dissociative attachment (DA),



and the H^- ion in the ion-pair formation (1P),



Here, E_e is the incident electron laboratory energy, $H(nl)$ are all energetically-open exit channels for the H atom, and E_p is the threshold for ion-pair formation into the ground state of H (1 7.322 eV). Using the methods outlined previously for the $e + NO$ system [23] one is able to identify in Eq. (1) the various open $H(nl)$ channels by measuring the kinetic energy of the outgoing H^- , and in Eq. (2) the simultaneous onsets of H^+ and H formation as a function of e/E_e .

In addition, three sources of positive ions were studied. The first channel is the proton in the IP process [Eq. (2)]. The second is production of H_2^+ by the direct ionization step,



And the third *via* dissociative ionization (DI),



Details, unique to the present work, of the magnetically-confined, trochoidal-analysis system, as well as the kinematics of the DA system, are given in *Sec. II*. Results are presented in *Sec. III*, and discussed in *Sec. IV* in terms of attachment (for the DA process) *via* the excited $V''J''$ levels, and in terms of the potential-energy curves involved in the three exit channels.

II. EXPERIMENTAL CONSIDERATIONS

A schematic diagram of the apparatus used to form the H^+ , H^- , and H_2^+ ions is shown in Fig. 1. The experiment is carried out within a uniform, 6T magnetic field. Electrons (e) are extracted from a hot, hairpin tungsten filament (F), accelerated to the desired final energy E_e in the range 3-30 eV, and attach to a beam of H_2 effusing from a 1 mm-diameter hypodermic needle. The emerging H^+ , H^- , and H_2^+ ions and parent-beam electrons are deflected in a trochoidal monochromator (TM). The faster electrons are deflected only several millimeter, and are collected in Faraday cup FC_e . The electric field of TM is swept linearly to velocity-analyze the ions. The transmitted ions spiral through two slits and a shielded transmission (TR) cage, then are detected in an analog mode in a second ion Faraday cup (FC_i). The ion current S is digitized and stored in a PC. Typical operating pressure near the H_2 beam is 6.5×10^{-5} Pa and at the detector FC_i , 6.5×10^{-7} Pa. The electron current ($\approx 10^{-7}$ A) and ion current ($\approx 10^{-11}$ A) were kept sufficiently low so that space-charge broadening effects in either beam were minimal (electrons) or absent (ions) [241].

III. RESULTS

Ion-energy spectra for the dissociative attachment process [Eq.(1)] are shown in Figs. 2-4. A spectrum corresponding to various positive-ion processes is shown in Fig. 5, and results for ion-pair formation shown in Fig. 6. These results are discussed separately in the following section.

Dissociative Attachment

As in the O/NO study [23], one treats the H and H^- fragments as emerging from a zero center-of-mass (CM) energy, The energy distribution of the outgoing H^- ion in Eq. (1) is given by [251

$$E_I = \frac{\mu}{m_H} \Delta E_{CM} + \cos\theta \sqrt{\frac{4\mu}{M} E. A E_{CM}} . \quad (5)$$

Here, E_I is the ion's laboratory energy, m_H is the atomic hydrogen mass, μ the reduced mass, and M the total H_2 mass. The angle θ is the CM angle of the outgoing H^- ion relative to the CM velocity along the incident H_2 direction. The initial (thermal) H_2 energy is E_o , and ΔE_{CM} is the total CM energy available to fragment translational. This quantity is given by

$$\Delta E_{CM} = \frac{\mu}{m_H} [E. + E_{v''j''}^* - (D_o^o - A + E^*)] , \quad (6)$$

where $E_{v''j''}^*$ is the vibration-rotation energy in the $H_2(X)$ state, D_o^o is its dissociation energy (3.7238 eV), A the electron affinity of H (0.7542 eV), and E^* the energy separation of states $H(n = 2,3...)$ relative to $H(n = 7)$. The effect of E_{vib}^* is to serve as a source of internal kinetic energy *via* vibration and rotation, just as the electron affinity A is a electronic potential-energy source. One may use Eqs. (5) and (6) to calculate the LAB energies of H^- and compare them to measurements.

Shown in Figs. 2-4 are experimental ion-energy spectra corresponding to the DA process given by Eq. (1). The three electron energies (4.0, 10.0 and 14.3 eV) were selected to correspond to the maxima in negative-ion production [1 ,2,7]. The

attachments at $E_e = 4.0$ eV (Fig. 2) and $E_e = 10.0$ eV (Fig. 3) are at electron energies below the $H(n = 2)$ threshold so that only a single peak is observed. The excitation at $E_e = 14.3$ eV is just above the opening of the $n=2$ channel. Hence one observes two H^- energy components corresponding to the H -atom in an $n=1$ or $n=2$ state. The shaded regions under each spectrum correspond to the range of LAB energies given by Eqs. (5) and (6) with θ taken in the entire CM interval $\{0, \pi\}$. An additional small broadening of ± 0.2 eV due to the estimated energy spread of the incident electron beam was also included in the calculated width.

One sees that the peaks in Figs. 2-4 are broader than can be accounted for by Eq. (5), whereas a similar analysis in NO was able to account for the majority of the measured O^- widths [231]. The additional broadening here was assumed to be due to the presence of vibrationally-excited H_2 molecules in the target region. While these densities are quite small (as low as 10^{15} the $v'' = 0$ population [20,221]), the variation of DA cross section $\sigma_{DA}(v'', J'')$ with v'' is quite steep, increasing by about a factor of 5-10 per vibrational level for the lower levels [3,9-1 1,1 9,22]. Hence the attachment rate from excited levels [proportional to the product *population* $\times \sigma_{DA}(v'', J'')$] can be comparable to the $v'' = 0$ rate.

To model the observed spectra the Boltzmann vibration-rotation population of H_2 levels at various, single vibration-rotation temperature $T = T_v = T_J$ was calculated. These populations were then used to weight the $\sigma_{DA}(v'', J'')$. A full set of experimental $\sigma_{DA}(v'', J'')$ was kindly provided by Popović et al. [191]. In more detail, the relative vibration-rotation population $f_{v'', J''} = N_{v'', J''} / N$ is given by the standard expression,

$$f_{v''J''} = \frac{(2J'' + 1) \exp -[(E_{v''} + E_{J''})/kT]}{Q_v Q_J}, \quad (7)$$

where Q_v and Q_J are the vibrational and rotational partition functions, respectively, $E_{v''}$ the vibrational energy (disregarding the zero-point energy, here and in Q_v), $E_{J''}$ the rotational energy, k the Boltzmann constant, and T the assumed molecular temperature. The ion current can then be expressed as

$$I(E_i) = C \sum_{v''J''} f_{v''J''} \times \sigma_{DA}(v'', J'') \times \exp \frac{-(E_i - E_{v''} - E_{J''})^2 4 \ln 2}{W^2}. \quad (8)$$

Here, W is the broadening (full-width at half-maximum) due to the resolution of TM, and is measured to be 0.61 the ion energy E_i [23]. The constant C describes other parameters such as electron current, H_2 gas density N , etc. which are not needed for this relative-intensity comparison.

One models the experimental results by assuming a series of Tin Eq. (7), then calculating *via* Eq. (8) the expected signal $I(E_i)$ relative to the peak signal in the experimental. The effect of the vibration-rotation energy is to extend the range of possible H^- energies to higher energies. This is clearly seen in Figs. 2-4. One also sees a sensitivity to the fits such that a single temperature of 1150 K would fit the DA results. Previous work had indicated two regimes of relaxation [19,20]. One corresponded to little $v''J''$ relaxation under conditions of H_2 low pressure. This gave different temperatures of $T_{v''} = 3000$ K and $T_{J''} = 550$ K. The second corresponded to $v''J''$ relaxation under conditions of high source pressure or large number of relaxing collisions, which gave closer temperatures $T_{v''} = 1800$ K and $T_{J''} = 1500$ K. Present

results correspond to a higher-relaxed regime, with results $T = T_v = T_J = 1150$ K. The relaxation is probably due to the fact that vibrationally-excited H_2 , formed at the tungsten filament (Fig. 1) must migrate about 7 cm towards TM, after which attachment cannot occur. At a chamber pressure of about 10^{-4} torr the mean free path for $H_2 - H_2$ collisions is 100 cm. Hence the excited H_2 are likely making multiple collisions with the lens walls (rather than with other molecules) to relax to low $v''J''$ populations.

Ion-Pair Formation

Measurements in the ion-pair production channel [Eq. (2)] were taken in separate runs by first tuning the electric field in TM to transmit the $m_H = 1$ particles (positively- and negatively-charged). The central grid of TR was then biased + 130 V to transmit H^- , and its energy width recorded. The grid in TR was then biased - 130 V to transmit H^+ , and its energy width recorded. The superimposed results are shown in Fig. 5 for an incident electron energy $E_e = 30$ eV. The difference in line shape for the H^+ and H^- ions is almost certainly related to differences in instrument contact potentials (hence acceleration energy) for the positive and negative charges; and to beam shear in the trochoidal monochromator (the top and bottom plates were not biased symmetrically about zero center-line voltage). The peak locations agree to within the experimental uncertainty of 0.02 eV; and the integrated counts in the two channels [76,407 (H^+) and 74,327 (H^-)] agree to 2.8%. These results indicate that there was no systematic discrimination by charge, and that outgoing ion energies had been correlated with the proper exit channel. This fact is used in the following

discussion for positive-ion formation.

Positive-Ion Formation

By biasing the center electrode of the transmitting cage TR negative, one may reflect all negatively-charged particles (ions and any electrons), and transmit only positively-charged ions. By sweeping the electric field in TM one can then obtain the energy spectrum of positively-charged particles. Shown in Fig. 6 are spectra taken at $E_e = 23$ eV and 30 eV. At both energies there are three open, positive-ion channels. In order of increasing thresholds these are: (a) direct ionization [(Eq. (3), threshold at 15.4259 eV], (b) IP formation [(Eq. (2) at 17.3225 eV], and (c) DI [(Eq. (4) at 18.0767 eV]. To explain the features we note that the lowest-energy feature should correspond to direct ionization, The lighter, outgoing electron leaves with approximately $30.0 - 15.4 = 14.6$ eV energy, with only the order me/M , or 10^{-2} eV, transferred to the heavier H_2^+ . The middle peak (b) corresponds to the IP process by virtue of the fact that its negative-ion partner falls at the same ion energy (Fig. 5). The third peak (c) must then correspond to the DI channel given by Eq. (5).

As a check on these channel assignments, a series of measurements were carried out in the vicinity of each threshold. It was found that peak (a) vanished at E_e less than 15.0 ± 0.5 eV, and peaks (b) and (c) both vanished at E_e less than 17.5 ± 0.5 eV. These values are consistent with the appropriate thresholds [12] (Table 1).

IV. DISCUSSION

To understand the observed low-energy ions produced in the DA, IP and DI processes one must appeal to the possible potential-energy curves involved. In the case of the lowest-energy DA channel, the $X^2\Sigma_u^+$ and $B^2\Sigma_g^+$ electronic states of H_2^- are involved [8,10,12]. The kinetic-energy distribution of H^- shown in Figs. 2-4 can be understood in terms of excitation to these states, and the kinematics *via* Eqs. (5) and (6), including the modeled $v''J''$ contribution. Total negative-ion production through these states (no energy analysis) has been seen in earlier work [1]. Some experimental and computational studies of the H^- energy and angular distributions have also been reported [4]. Energetic protons produced *via* H_2^+ and autoionizing H_2 states have been reported by Köllmann [51] and Landau *et al.* [6].

Dissociative Attachment

Production of H^- *via* DA proceeds through the resonance states $X^2\Sigma_u^+$ and $B^2\Sigma_g^+$ of H_2^- . The expected ion kinetic-energy distribution is shown as the shaded regions in Fig. 2-4 at incident electron energies $E_e = 4.0, 10.0$ and 14.3 eV, respectively. In each case the H^- production extends to higher energies than calculated by Eqs. (5) and (6) (with $E''_{v''J''} = 0$). This additional energy arises through $V''J''$ excitation in the ground state, with a distribution described by an effective vibration-rotation temperature. Shown in Figs. 2-4 are ion energy distributions calculated for three different vibration-rotation temperatures T . A single T of approximately 1150 K adequately describes the data. This temperature is lower than

the $T_V \approx 1800$ K observed in Ref. 10. The difference could be explained by more extensive vibrational-rotation quenching in the present instrument geometry (Fig. 1), due to the long path between the region of $H_2(v'', J'')$ formation (near F), and the entrance to TM.

Ion-Pair Formation

Shown in Fig. 5 are separate spectra taken with TR biased negative (H^+ transmission-detection), and positive (H^- transmission-detection). Of interest here are (a) the ion signals appear, as expected, in the same energy interval, (b) the integrated counts for each charge state are equal, and (c) the ions appear at low energies. Points (a) and (b) confirm the fact that the an ion-pair exit channel is being detected, and (c) arises from the fact the H_2 electronic state(s) involved are being excited close to threshold, near the $H^+ + H^-$ asymptote of 17.3225 eV (Fig. 7). This energy location is helpful in identifying the exit channels in the positive-ion spectrum (see below).

From the molecular-orbital correlation diagram [12, 13] the states which can lead to ion-pair production are of $^1\Sigma_u^+$ symmetry. These include also $^1\Sigma_u^+$ states which correlate to the limits $H(1s) + H(n = 2-4)$, and which are embedded in the $H^+ + H^-$ dissociation continuum. Two of these states have been proposed as strong contributors to ion-pair production in photoabsorption [13]. They are the $H_2 B''$ [12] and $4f\sigma$ [14] states. These states, along with the $2p\sigma B^1\Sigma_u^+$ and $3p\sigma B'^1\Sigma_u^+$ states as possible contributors, are shown in Fig. 7.

Positive-ion Formation

The positive-ion energy spectrum is shown in Fig. 6 at incident electron energies of 23 eV and 30 eV. The identification of the features proceeded as follows. Feature (b) appears at the same energy location as in Fig. 5, hence it must correspond to H^+ resulting from ion-pair production through the $^1\Sigma_u^+$ symmetry states. Feature (c) must also be due to H^+ , since there can be no sources of energetic H_2^+ in this system. Feature (a) correspond to thermal H_2^+ formed by direct ionization of H_2 [Eq. (3)]. This is consistent with its low energy — corresponding to negligible momentum transfer between the electron and thermal (0.04 eV) H_2 — and the disappearance of this peak at E_e below 15.0 ± 0.5 eV. Thermal H_2^+ formation arises by direct excitation to the $X\ ^2\Sigma_g^+$ state over a broad range of Franck-Condon factors.

Another property of the positive-ion behavior in Fig. 6 is that the shapes and energy positions of peaks (b) and (c) are unchanged at the two electron energies. Referring to Fig. 7, this is consistent with excitation to the repulsive edges of the potential-energy curves asymptotic to the IP and DI thresholds (shown through the shaded, left-hand Franck-Condon region in Fig. 7). For the ion-pair peak (b) excitation can be through the B'' and $4f\sigma$ H_2 states. For Peak (c) DI can occur through excitation to the repulsive wall of the H_2^+ X state. Kinetic energies derived from the shaded region and the asymptotic energies are in very good agreement with the ion energies of Fig. 6, when one takes into account that excitation can be from several excited v'' levels in the ground state, to steeply-rising portions of the curves in the upper state. Furthermore, one also sees that the Franck-Condon overlap between $v'' = 0$ in the H_2 X state and the dissociating states is negligible. Hence, excitation to the states must

be taking place through levels $v'' \geq 1$, which have been populated presumably by the wall-recombination mechanism described above.

V. ACKNOWLEDGEMENTS

We thank C. Schermann for providing us with measured DA cross sections for $H_2(v'',J)$. We also thank J. Greenwood for a helpful discussion. This work was carried out at the Jet Propulsion Laboratory, California Institute of Technology, and was supported by the National Aeronautics and Space Administration.

References

- [11] G. J. Schulz, *Phys. Rev.* 713, 816(1959); G. J. Schulz and R. K. Asundi, *Phys. Rev.* 758, 25 (1 967).
- [2] D. Rapp, T. E. Sharp and D. D. Briglia, *Phys. Rev. Lett.* 74, 533 (1 965).
- [31] M. Allan and S. F. Wong, *Phys. Rev. Lett.* 47, 1791 (1978).
- [41] M. Tronc, F. Fiquet-Fayard, C. Schermann and R. I. Hall, *J. Phys. B: Atom. Mol. Phys.* 10, 304 (1 977); M. Tronc, R. I. Hall, C. Schermann and H. S. Taylor, *J. Phys. B: Atom. Mol. Phys.* 12, L279 (1979).
- [51] K. Köllmann, *J. Phys. B: Atom. Molec. Phys.* 71, 339 (1 978).
- [6] M. Landau, R. I. Hall and F. Pichou, *J. Phys. B: Atom. Molec. Phys.* 74, 1509 (1981).
- [7] S. K. Srivastava and O. J. Orient, in *Production and Neutralization of Negative Ions and Beams* (ed. K. Prelec, Am. Inst. Phys., NY, 1984) p.56.
- [81] J. N. Bardsley and J. S. Cohen, *J. Phys. B: Atom. Molec. Phys.* 77, 3645 (1978).
- [9] J. N. Bardsley and J. M. Wadehra, *Phys. Rev. A* 20, 1398 (1 979).
- [10] J. M. Wadehra, in *Nonequilibrium Vibrational Kinetics* (ed. M. Capitelli, Springer, New York, 1986), Ch. 7.
- [11] A. P. Hickman, *Phys. Rev. A* 43, 3495 (1991),
- [12] T. E. Sharp, *Atomic Data* 2, 119 (1971).
- [13] W. A. Chupka, P. M. Dehmer and W. T. Jivery, *J. Chem. Phys.* 63, 3929 (1 975).
- [14] E.R. Davidson, in *Physical Chemistry, An Advanced Treatise, V. III* (ed. D. Henderson, Academic, New York 1969) Ch.3; and private communication (1997).
- [15] D. A. Skinner, A. M. Bruneteau, P. Berlemont, C. Courteille, R. Leery and M.

- Bacal, *Phys. Rev. E* 48, 2122 (1993).
- [16] J. R. Hiskes and A. M. Karo, *J. Appl. Phys.* 67, 6621 (1990); J. R. Hiskes, *Rev. Sci. Instr.* 63, 2702 (1992).
- [17] Yu. Belchenko, *Rev. Sci. Instr.* 64, 1385 (1993).
- [18] M. Bacal, C. Michaut, L. 1. Elizarov and F. El Balghiti, *Rev. Sci. Instr.* 67, 1138 (1996).
- [19] D. Popović, 1. Čadež, M. Landau, F. Pichou, C. Schermann and R. 1. Hall, *Meas. Sci. Technol.* 7, 1041 (1990).
- [20] R. 1. Hall, 1. Čadež, M. Landau, F. Pichou and C. Schermann, *Phys. Rev. Letters* 60, 337 (1988).
- [21] 1. Čadež, C. Schermann, M. Landau, F. Pichou, D. Popović and R. 1. Hall, *Z. Phys. D* 26, 328 (1993).
- [22] S. Gough, C. Schermann, F. Pichou, M. Landau, 1. Čadež and R. 1. Hall, *Astron. Astrophys.* 305, 687 (1993).
- [23] O. J. Orient and A. Chutjian, *Phys. Rev. Letters* 74, 5017 (1995).
- [24] O. J. Orient, A. Chutjian, K. E. Martus and E. Murad, *Phys. Rev. A* 48, 427 (1993).
- [25] F. Brouillard and W. Claeys, in *Physics of Ion-Ion and Electron-Ion Collisions* (ed. F. Brouillard and J. Wm. McGowan, Plenum, New York, 1983), p. 415.
- [26] K. P. Huber and G. Herzberg, *Molecular Spectra and Molecular Structure IV. Constants of Diatomic Molecules* (Van Nostrand Reinhold, New York 1979).

Table 1. Energies of H₂ (to 0.001 eV) relative to H₂ X (*v*"=0, *J*"=0) [1 2].

Limit	Energy (eV)
<i>H</i> ⁻ (1 <i>s</i> ²) + <i>H</i> (1 <i>s</i>)	3.724
<i>H</i> (1 <i>s</i>) + <i>H</i> (1 <i>s</i>)	4.478
<i>H</i> ⁻ (1 <i>s</i> ²) + <i>H</i> (2 <i>l</i>)	13.922
<i>H</i> (1 <i>s</i>) i- <i>H</i> (2 <i>l</i>)	14.676
<i>H</i> ₂ ⁺ X (<i>v</i> "=0, <i>J</i> "=0)	15.426
<i>H</i> ⁻ (1 <i>s</i> ²) + <i>H</i> ⁺	17.322
<i>H</i> ⁺ i- <i>H</i> (1 <i>s</i>)	18.076

Figure Captions

Figure 1.

Schematic diagram (not to scale) of the magnetically-confined trochoidal system. Electrons (e) from a filament (F) attach or excite H_2 to form H^+ , H^- , or H_2^+ ions. The electron energy range is 3-10 eV. The ions and electrons are separated by the trochoidal monochromator (TM), which also analyzes the different ion velocities as its electric field is swept. The velocity-analyzed ions spiral to the transmission cage TR where the sign of charge is selected by the potential on the central grid. The analog ion signal S is detected at FC.

Figure 2.

Dissociative attachment $I-I$ energy spectrum for 3.8 eV incident electron energy. The spectrum is modeled in terms of a rotation-vibrational population at the indicated temperature T and the DA cross sections from Ref. 10. All curves are normalized to the peak of the experimental signal. The shaded interval is the expected peak width in the absence of $v''J''$ excitation, calculated from Eqs. (5) and (6) ($E_{v''J''=0}^*$).

Figure 3.

Same as Fig. 1, but at an incident electron energy of 10.0 eV.

Figure 4.

Dissociative attachment H^- energy spectrum for 14.3 eV incident electron energy. Modeling calculations areas in Fig. 1. The intervals indicated are the expected peak widths with $E_{v,J}^* = 0$, calculated for the final atomic states $H(n=1)$ and $H(n=2)$.

Figure 5.

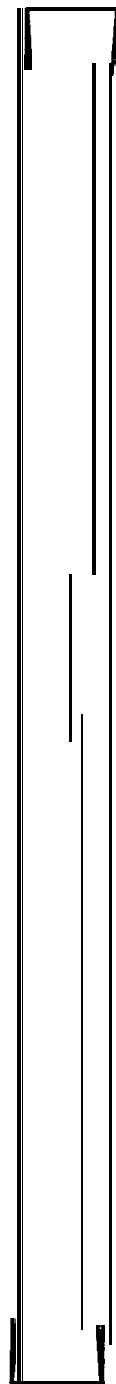
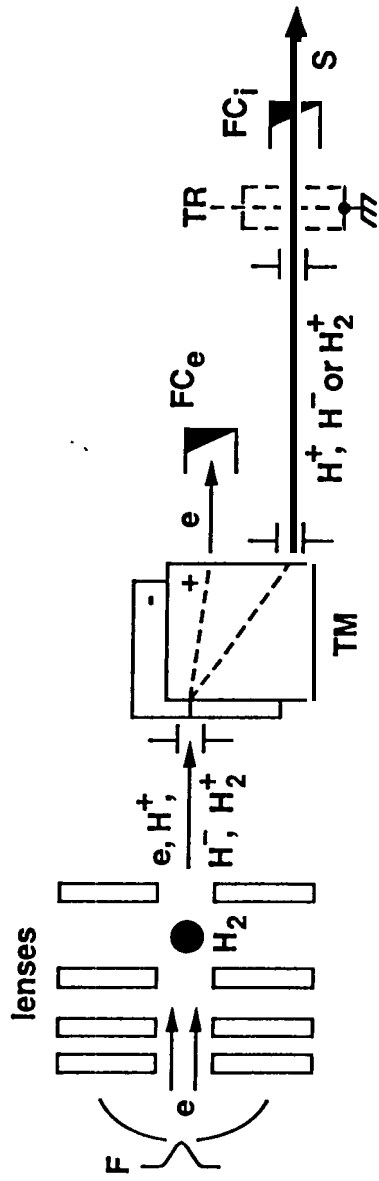
Experimental detection of the ion-pair production channel for electron-impact dissociation of H_2 at 30 eV electron energy. The distortion in line shapes is very likely due to contact-potential differences and beam shear in the trochoidal monochromator. The integrated signals of H^+ and H^- particles agree to 2.8%.

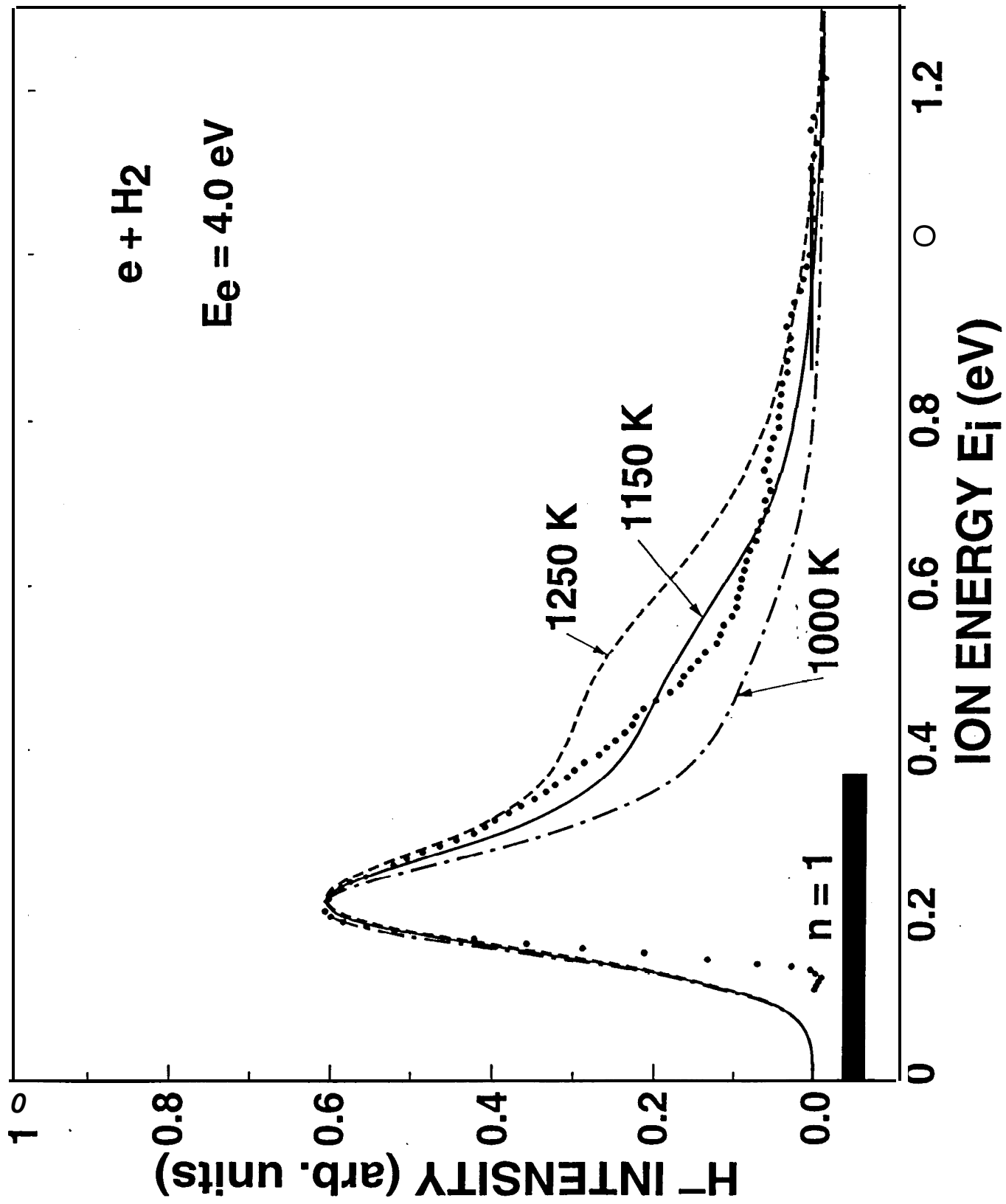
Figure 6.

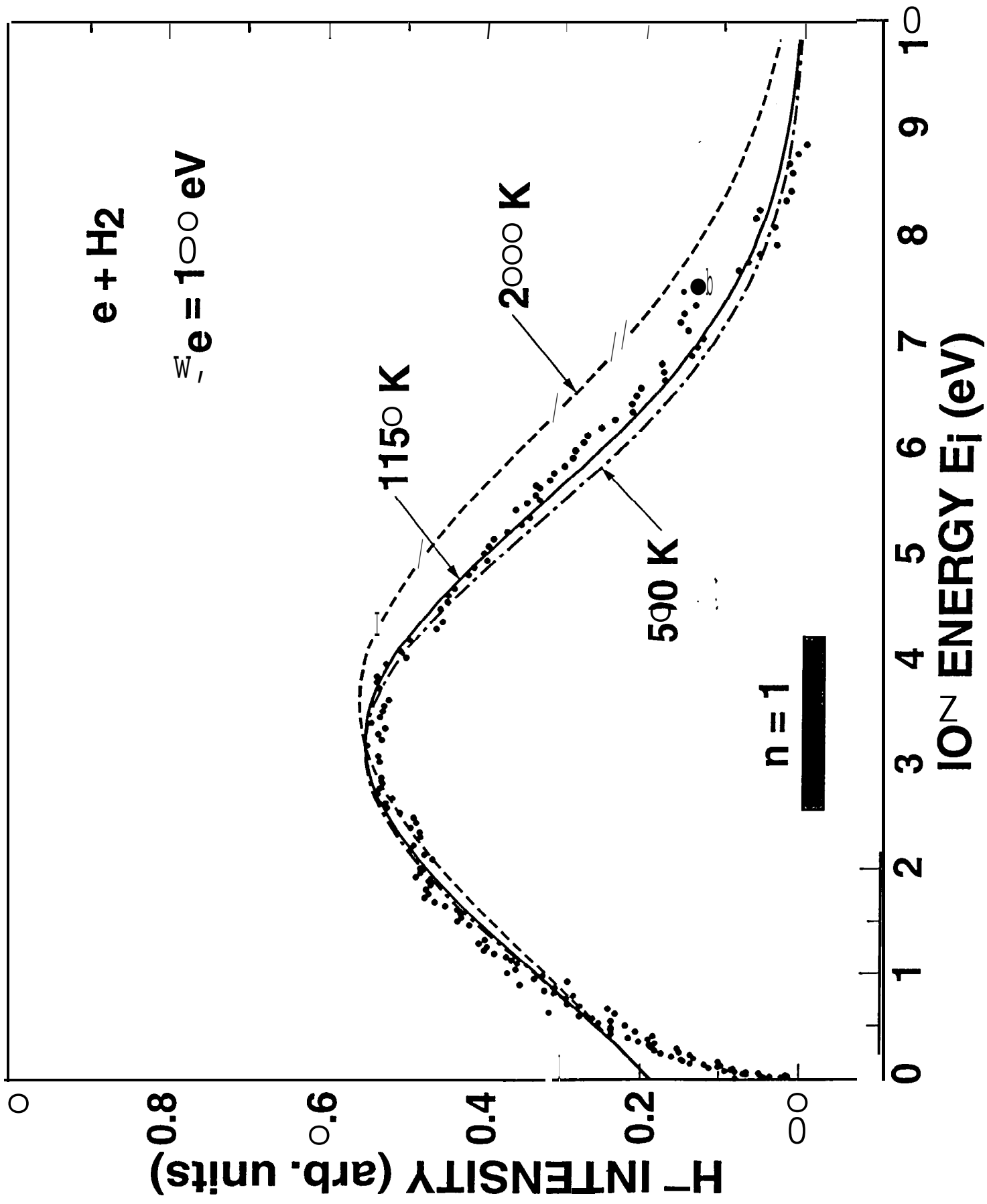
Energy spectrum of positive ions following electron-impact excitation of H_2 at incident electron energies of 23 eV (open circles) and 30 eV (filled circles). The three labeled peaks are the channels: (a) $e + H_2 \rightarrow H_2^+ + e$ (direct ionization), (b) $e + H_2 \rightarrow H^+ + H^- + e$ (ion-pair formation), and (c) $e + H_2 \rightarrow H(n=1) + H^+ + e$ (dissociative ionization).

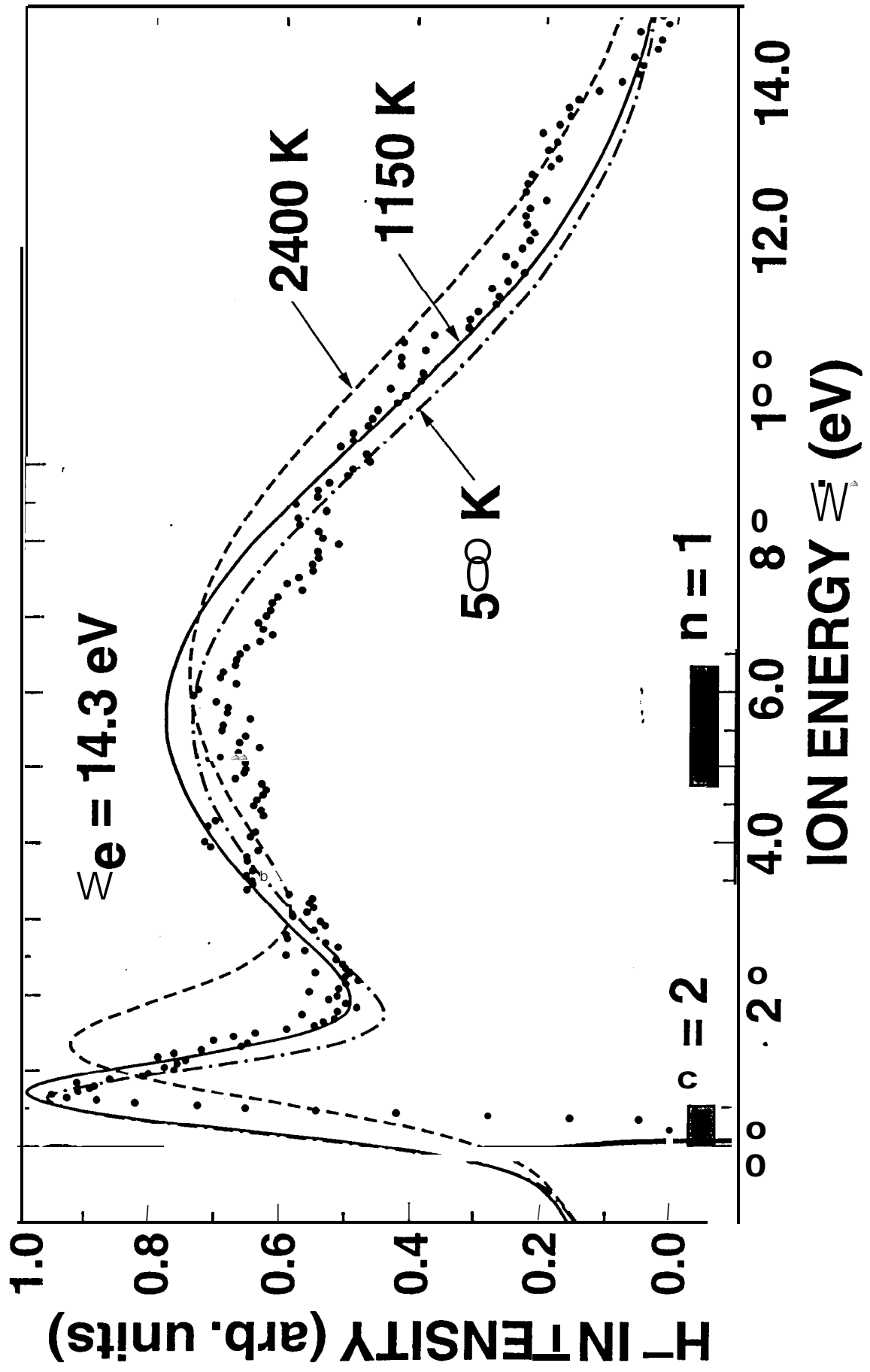
Figure 7.

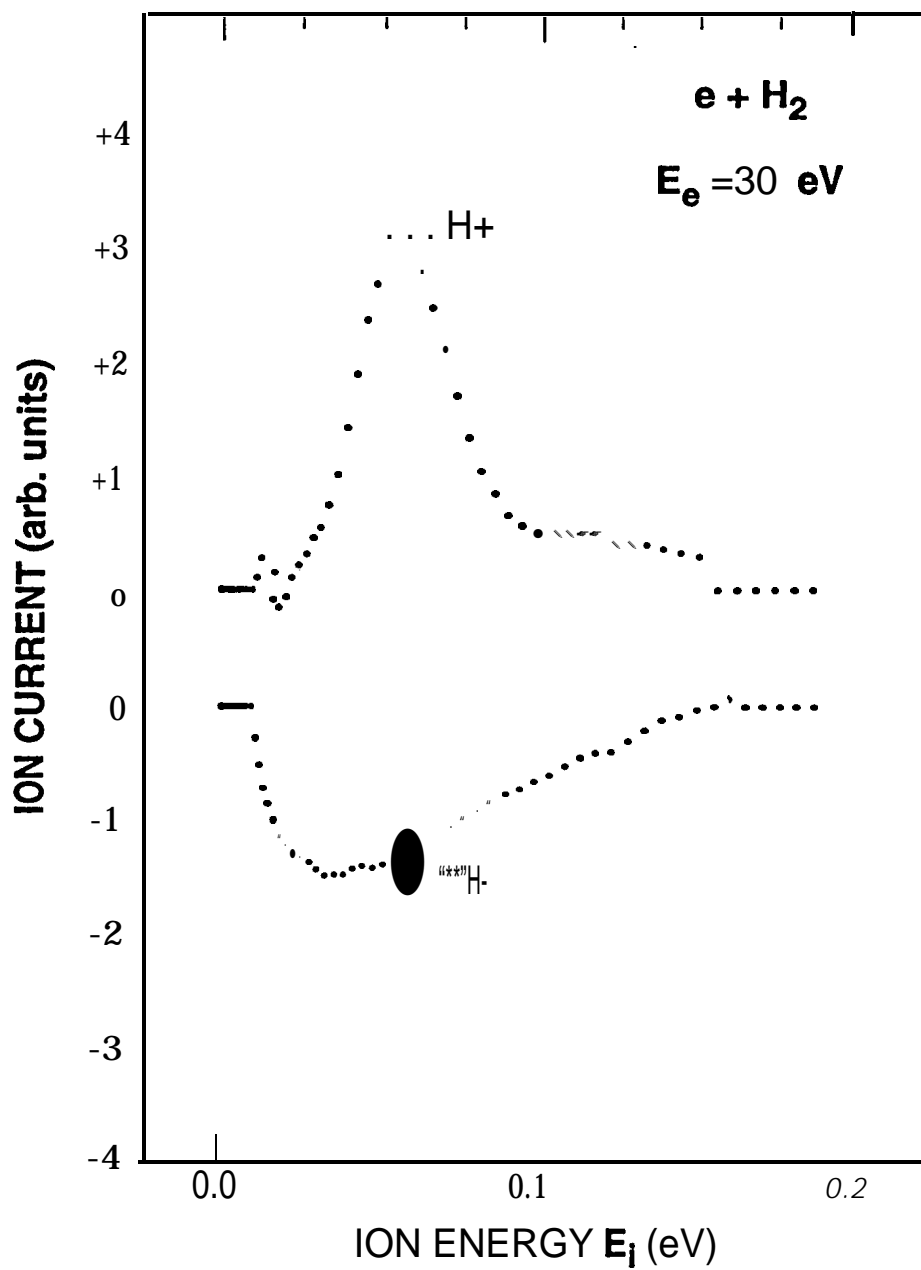
Partial potential-energy diagram for H_2 showing the relevant electronic states and asymptotic limits. The $H_2^+ X^2\Sigma_g^+$ state is taken from Sharp [12], and the $4f\sigma^+ 1\Sigma_u^+$ state is from unpublished results of Davidson [14],

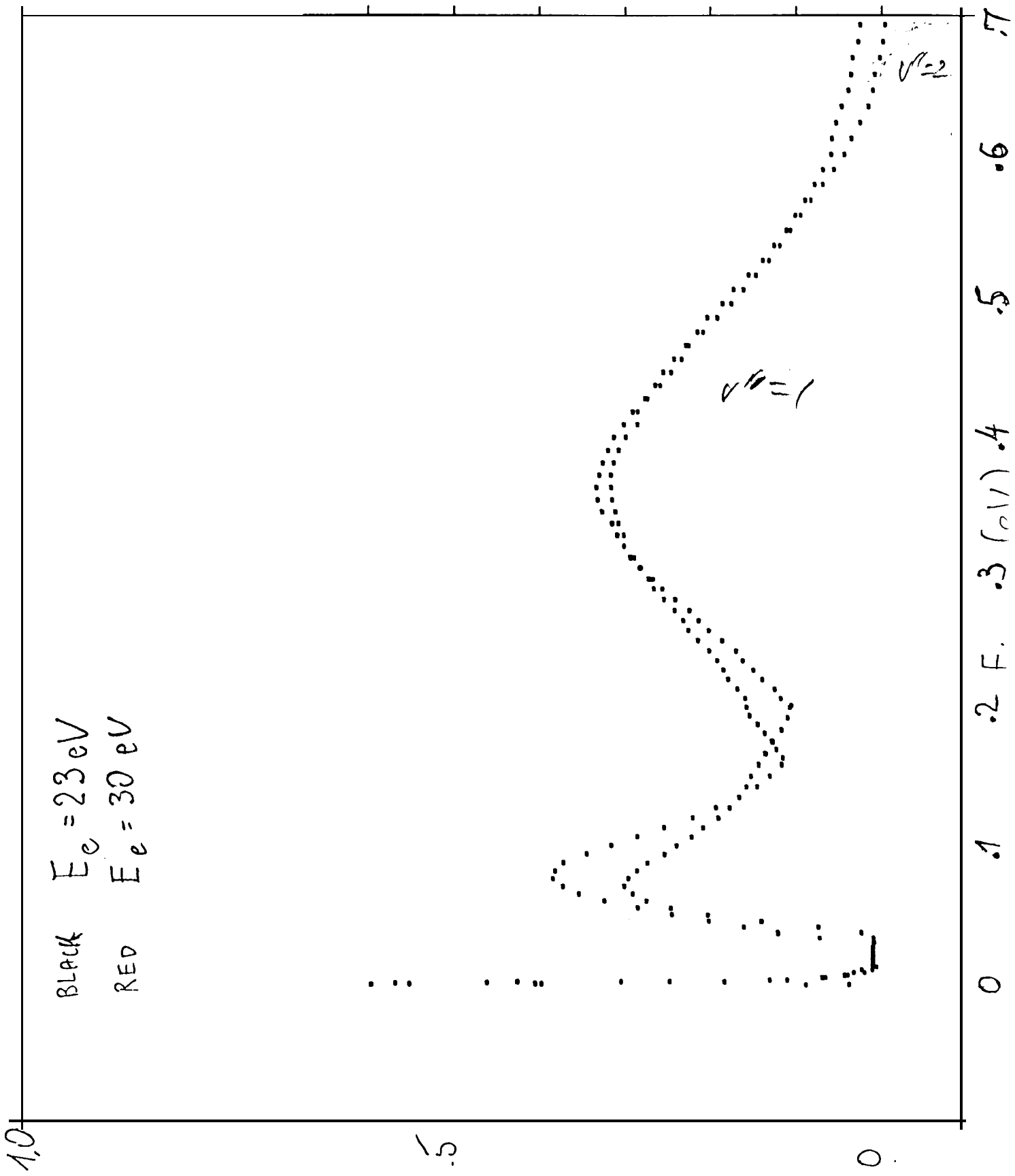


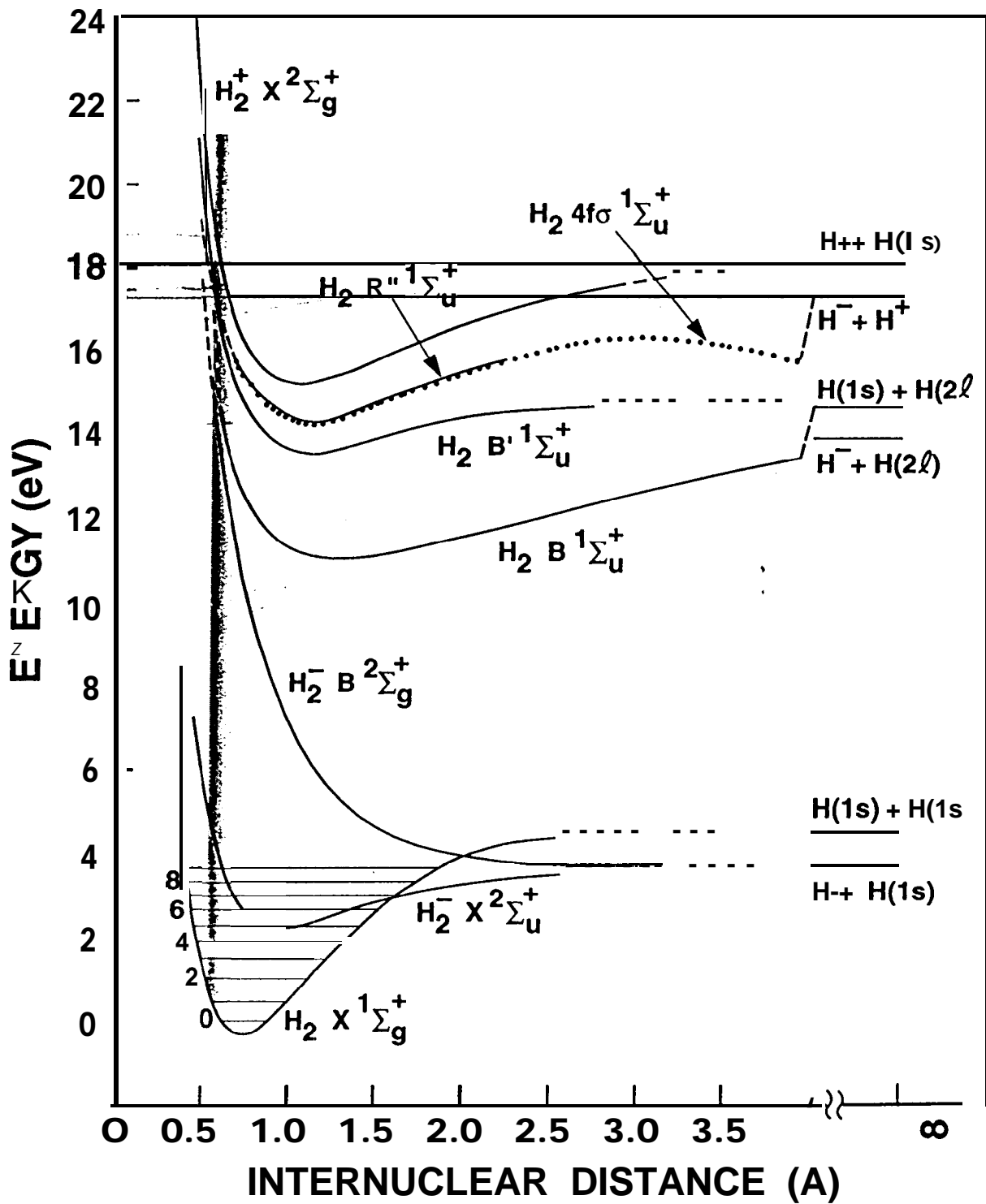












18